

Effects of Extended Surfactant Structure on the Interfacial Tension and Optimal Salinity of Dilute Solutions

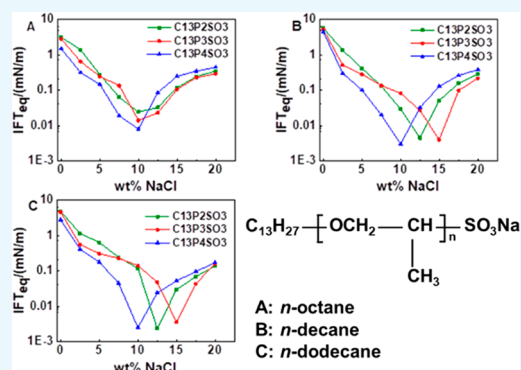
Weidong He,^{*,†,§} Jijiang Ge,^{*,†} Guicai Zhang,^{†,‡} Ping Jiang,[†] and Luchao Jin^{†,||}

[†]College of Petroleum Engineering and [‡]State Key Laboratory of Heavy Oil Process, China University of Petroleum, Qingdao, Shandong 266580, P. R. China

[§]SINOPEC Research Institute of Safety Engineering, Qingdao, Shandong 266100, P. R. China

^{||}Alchemy Sciences Inc., Houston, Texas 77072, United States

ABSTRACT: Extended surfactants with the oxypropylene (PO) group and ethoxylated anionic surfactants with the oxyethylene (EO) group have a high salt tolerance capability. Most of the researches on extended surfactants and ethoxylated anionic surfactants focused on the microemulsion, solubilization, and interfacial tension (IFT) of concentrated surfactant solutions, whereas a few researches focused on the IFT of dilute surfactant solutions. Moreover, a previous work focused only on surfactants with PO numbers greater than 4 and copolymers of PO and EO. The effects of extended surfactants containing short PO chains and no EO groups have not been examined. We measured the IFT and optimal salinity between *n*-alkanes and dilute solutions of extended surfactants or ethoxylated sulfonates at 30 °C. The effects of the surfactant structure on the equilibrium interfacial tension (IFT_{eq}) and optimal salinity of the system were studied in detail. As for the effects on IFT, results indicate that the introduction of PO groups leads to their enhanced capability to reduce the IFT prior to cross-salinity and a reduction in the IFT between *n*-alkanes and surfactant solutions to ultralow values (smaller than 0.01 mN/m) near the optimal salinity. It was also found that extended surfactants with different alkyl chains also entail a cross-salinity; at values lower than the cross-salinity, the IFT reduction capacity of extended surfactants with a long alkyl chain (C16P3SO3) is better than that of extended surfactants with a short alkyl chain (C13P3SO3). As for the effect on the optimal salinity, it was found that the optimal salinity of extended surfactants is lower than that of ethoxylated sulfonates for the same oil phase. It was also found that the optimal salinity of extended surfactants first increased and later decreased with increasing PON. This finding is first proposed based on summarizing some researchers' studies and our experiments.



INTRODUCTION

In the petroleum industry, surfactants play a very important role in the chemical flooding technology for enhancing oil recovery (EOR) due to their capability of reducing interfacial tension. Besides surfactant flooding, surfactants can be used in many chemical combination flooding systems, such as surfactant/polymer,^{1–3} alkaline/surfactant/polymer,^{4–6} and surfactant/alkaline^{7–9} systems. Two distinct mechanisms in reducing interfacial tension with surfactants have been found. The first mechanism involves the aggregation of many surfactant molecules at the brine–oil interface where the tension reaches the minimum at a surfactant concentration under 1 wt %.^{10,11} The second mechanism occurs when a surfactant-rich microemulsion phase forms at a surfactant/cosurfactant concentration above 1 wt % and a low tension appears at the microemulsion–brine interface or at the microemulsion–oil interface, or at both if both are present.^{12,13}

Petroleum sulfonate and alkyl-benzene sulfonate are two classical surfactants used in chemical flooding. The polar hydrophilic head and nonpolar lipophilic tail of these surfactants are directly connected by a chemical bond. The

salt tolerance of this type of surfactants is so low that solutions of these species become unstable and phase separation occurs under high-salinity conditions (beyond 2 or 2.5 wt % NaCl¹⁴). The optimal salinity of NaCl is in the range of 1–2 wt %.¹⁵ As a result, these surfactants are not efficient for the exploitation of high-salinity oil fields. For exploiting high-salinity oil fields, some researchers found that introducing a junction unit, such as oxyethylene (EO) groups and oxypropylene (PO) groups, between the hydrophilic head and lipophilic tail is expected to improve the interfacial performance and salt tolerance capacity of surfactants. By inserting EO groups or PO groups, two kinds of surfactants were invented: one comprised ethoxylated anionic surfactants with only EO groups between the hydrophilic head and the lipophilic tail; the other comprised so-called extended surfactants with PO groups or PO–EO groups.

Received: February 21, 2019

Accepted: July 4, 2019

Published: July 22, 2019

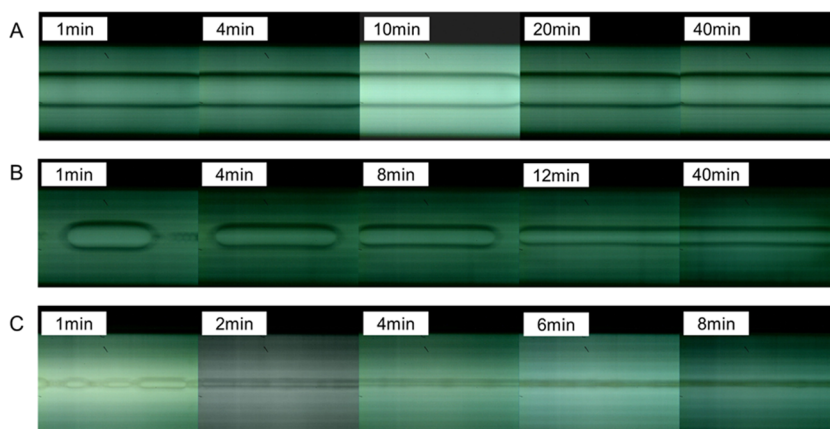


Figure 1. Morphology of *n*-alkane droplets changing with time in C13P2SO₃ solutions with different salinities: *n*-octane droplet in 2.5 wt % NaCl (A), *n*-octane droplet in 7.5 wt % NaCl (B), and *n*-decane droplet in 10 wt % NaCl (C).

Ethoxylated anionic surfactants were first developed in the 1930s.¹⁶ Since then, there was a dramatic increase of research on the phase behavior, solubilization, and application in the oil-field exploitation of high-concentration (more than 1 wt %) ethoxylated anionic surfactant solutions, especially ethoxylated sulfonates. Bansal et al.^{14,15} found that the addition of ethoxylated sulfonates can extend the use of petroleum sulfonates at a higher salinity (18 wt % NaCl to even 32 wt % NaCl), keeping the total surfactant concentration constant at 5 wt %. Skauge et al.,¹⁷ Abe et al.,¹⁸ and Miller et al.¹⁹ found that (i) branching of the alkyl chain reduces the optimal salinity and solubilization parameter, (ii) the benzene ring is equivalent to three methylene groups with respect to optimal salinity and solubilization, (iii) increasing the EON can increase the optimal salinity at a high degree of ethoxylation (EON > 3), whereas at low degrees of ethoxylation, the solubilization parameter increases and the optimal salinity decreases. Besides the high-surfactant-concentration condition, Aoudia et al.²⁰ measured the dynamic IFT of dilute surfactant solutions (0.1 wt %) and performed some core flooding experiments.

Extended surfactants are composed of some intermediate polarity groups, such as PO groups or PO–EO groups, which are inserted between the hydrophilic head and the lipophilic tail. Alkyl sulfate-extended surfactants were initiated and applied for EOR by the Exxon Production Research Company in the 1980s.²¹ Since then, abundant tests emerged and tended to be more popular for applications involving the interfacial properties, capability of forming microemulsions, and solubilization of surfactant solutions with a high surfactant concentration (more than 1 wt %) for long-chain alkanes, triglycerides, vegetable oils, and crude oils. These experimental results indicate that extended surfactants have the capability of forming middle-phase microemulsions with high solubilization^{22–26} and an ultralow IFT²⁶ for a wide range of oils. The studies also indicated that PO groups can extend the lipophilic portion into the deeper part of the oil phase near the interface without sacrificing the water solubility and form a smooth polarity-transition zone between the hydrocarbon and aqueous phases. As a result of the increasing PON, the solubilization increased and the optimal salinity, critical micelle concentration (CMC), and IFT decreased. Meanwhile, a few researchers measured the dynamic IFT between different oils and dilute extended surfactant solutions (e.g., 0.1,^{27,28} 0.2,²⁹ and 0.3 wt %^{30,31}), with the following findings: (i) these

extended surfactants can achieve an ultralow IFT with a wide range of oils, including highly hydrophobic oils (e.g., hexadecane), triglycerides, triolein, and vegetable oils, using only ppm levels of these extended surfactants;^{27–30} (ii) the introduction of PO groups in the extended surfactant yielded a lower optimal salinity^{28–30} and a linear correlation with the properties of the extended surfactants, such as a decreasing $\log(\text{CMC})$, a decreasing surface tension, and a decreasing $\ln S^*$ ³¹ (the optimal salinity for achieving an ultralow IFT); (iii) increasing the degree of tail branching can decrease the IFT;²⁸ and (iv) when the tail length of the surfactant is smaller, the optimal salinity increases.²⁹ However, one of the limitations of sulfate surfactants is their poor hydrolytic stability;³² new extended surfactants with sulfonate as the head group were studied recently. Guo et al.³³ measured the dynamic IFT between *n*-alkanes and solutions of four types of alkyl sulfonate-extended surfactants with PO–EO groups and concluded that the ratio of PON to EON is a key factor for controlling interfacial properties.

As described above, most of these researches focused on the microemulsion, solubilization, and IFT of concentrated surfactant solutions of ethoxylated sulfonates and sulfate-extended surfactants, and a few researches focused on the IFT of dilute sulfonate-extended surfactant solutions. Moreover, there is no report on the comparison of the properties of sulfonate-extended surfactants and ethoxylated sulfonates. Although the effect of PON on extended surfactant properties has been extensively studied, most of the studies focused on copolymers of PO and EO and a PON greater than 4. The effects of an extended surfactant structure with a short PO chain and no EO group have not been studied yet.

In this paper, we synthesized one ethoxylated sulfonate and four extended surfactants with sulfonate as the hydrophilic head, different PONs, and different lipophilic tails. We measured dynamic IFTs between *n*-alkanes and different surfactant solutions and studied the effects of the surfactant molecular structure, such as the PO group, alkyl chain length, and alkane carbon number, on the equilibrium IFT and optimal salinity. All of the salinities refer to the mass percent only in terms of NaCl.

RESULTS AND DISCUSSION

Morphology Change of *n*-Alkanes and Determination of IFT_{eq}. Figure 1 shows that the morphology of *n*-

alkanes changes with time under different experimental conditions. In Figure 1A, the morphology of the *n*-octane droplet was constant, and so the IFT remained at equilibrium in the beginning. In Figure 1B, the shape of the *n*-octane droplet was stretched with time, and then remained consistent, and so the IFT reached the equilibrium value after a certain time. In Figure 1C, the *n*-decane droplet split into multiple oil droplets due to an ultralow IFT. Then, the smaller oil droplets stretched quickly at an ultralow IFT, and subsequently split into many smaller droplets.

We chose the average IFT under equilibrium conditions as the IFT_{eq} . The IFT_{eq} values between different *n*-alkanes and C13P2SO3 solutions are shown in Figure 2. The values

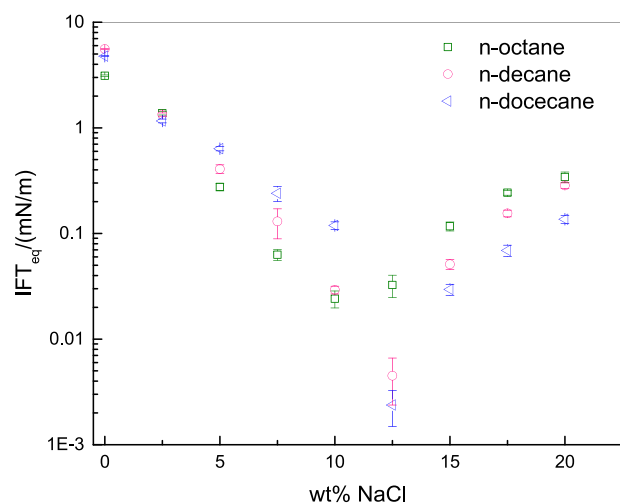


Figure 2. IFT_{eq} between *n*-alkanes and the solutions of C13P2SO3.

represent the average of two independent experiments. The standard deviations are smaller than 6%, especially smaller than 1% because the IFT_{eq} is very small at 7.5, 10, and 12.5 wt % NaCl.

Effects of PO and EO. Figure 3 compares the effects of PO and EO on the IFT_{eq} between *n*-alkanes and solutions of C13E3SO3 or C13P3SO3. As shown in Figure 3, the IFT_{eq} curves for C13P3SO3 and the IFT_{eq} curves for C13E3SO3 cross each other. When the concentration of NaCl is lower than that at the cross-salinity, the IFT_{eq} between *n*-alkanes and C13P3SO3 solutions is lower than that between *n*-alkanes and C13E3SO3 solutions. When the salinity is higher than the cross-salinity, the IFT_{eq} between *n*-alkanes and C13P3SO3 solutions is higher than that between *n*-alkanes and C13E3SO3 solutions. Moreover, the optimal salinity of C13P3SO3 is lower than that of C13E3SO3.

According to the surfactant assignment model,³⁴ the IFT_{eq} mainly depends on the number of molecules and the adsorption strength of the surfactant on the oil–water interface. As more surfactant molecules adsorb on the oil–water interface, and when the adsorption strength increases, the resulting IFT becomes lower. Additionally, under any given condition, the adsorption rate and adsorption strength of the surfactant molecules on the oil–water interface are related to the hydrophilic–lipophilic balance. The hydrophilicity and lipophilicity of common groups are shown in Table 1.³⁵

The sulfonic group is highly hydrophilic; the PO group is weakly lipophilic, and the EO group is hydrophilic. As a result, the introduction of PO groups to displace the EO groups can

improve the lipophilicity and the adsorption capability of the surfactant molecules on the oil–water interface.

Figure 4 shows the effect of salinity on the distribution of the surfactant in oil/water phases. According to the surfactant assignment model and the hydrophilicity and lipophilicity of common groups, C13E3SO3 molecules disperse more easily in the water phase and more C13P3SO3 molecules adsorb on the oil–water interface at a low salinity as shown in Figure 4A. Under this condition, the IFT_{eq} between oil and the C13P3SO3 solution is lower than that between oil and the C13E3SO3 solution. As the salinity increases, salinity can compress the thickness of the ion atmosphere of ionic surfactants and damage the peripheral hydration film of the hydrophilic group, reducing the hydrophilicity of the surfactant and allowing the molecules to gradually diffuse into the oil phase from the water phase, through the interface between the phases. Because of C13P3SO3 molecules' higher lipophilicity, C13P3SO3 molecules reach the maximum amount at the interface between the phases ahead of C13E3SO3 molecules, and the salinity reaches the optimal value for C13P3SO3 as shown in Figure 4B; the distribution of C13P3SO3 molecules in different phases is in equilibrium, which causes the IFT_{eq} to reach its lowest value. As shown in Figure 4C, as the salinity continues to increase, a considerable number of C13P3SO3 molecules diffuse into the oil phase, and amount of C13E3SO3 molecules continues to adsorb at the interface between the phases. There is an adsorption condition that the IFT_{eq} of each oil–water system is equal at the cross-salinity as shown in Figure 3. When the distribution of the C13E3SO3 molecules approaches equilibrium with increasing salinity, the salinity of C13E3SO3 reaches the optimal value as shown in Figure 4D and the IFT_{eq} between oil and the C13E3SO3 solution reaches the lowest value.

Additionally, the result that the optimal salinity of C13P3SO3 is significantly lower than that of C13E3SO3 also can be explained by the Winsor *R* ratio theory.^{17,29} According to the Winsor *R* ratio theory, there are three blocks in the oil–water system, including the water region (W), oil region (O), and amphiphilic region (C), as shown in Figure 5. The amphiphilic region is defined as a layer of surfactant molecules with a certain thickness and binary hydrophobicity. In this layer, the hydrophilic portion of the surfactant infiltrates into the water phase, whereas the lipophilic portion infiltrates into the oil phase. The intermolecular interactions existing in the amphiphilic region are expressed by cohesive energy *A*.

On the side of the lipophilic group layer, A_{oo} is the cohesive energy between oil molecules, A_{ll} is the cohesive energy between lipophilic groups, and A_{lco} is the cohesive energy between the lipophilic group and the oil molecule. On the side of the hydrophilic group layer, A_{ww} is the cohesive energy between water molecules, A_{hh} is the cohesive energy between hydrophilic groups, and A_{hcw} is the cohesive energy between the hydrophilic group and the water molecule. Additionally, A_{lcw} is the interaction between the lipophilic group and the water molecule. A_{lco} is the interaction between the hydrophilic group and the oil molecule. The cohesive energy A_{co} between the whole surfactant molecule and the oil molecule is the sum of A_{lco} and A_{hco} . The cohesive energy A_{cw} between the whole surfactant molecule and the water molecule is the sum of A_{hcw} and A_{lcw} . Because A_{lcw} and A_{hco} are very weak compared to the other cohesive energies, they can be ignored. Then, the definition of *R* ratio is presented in eq 1

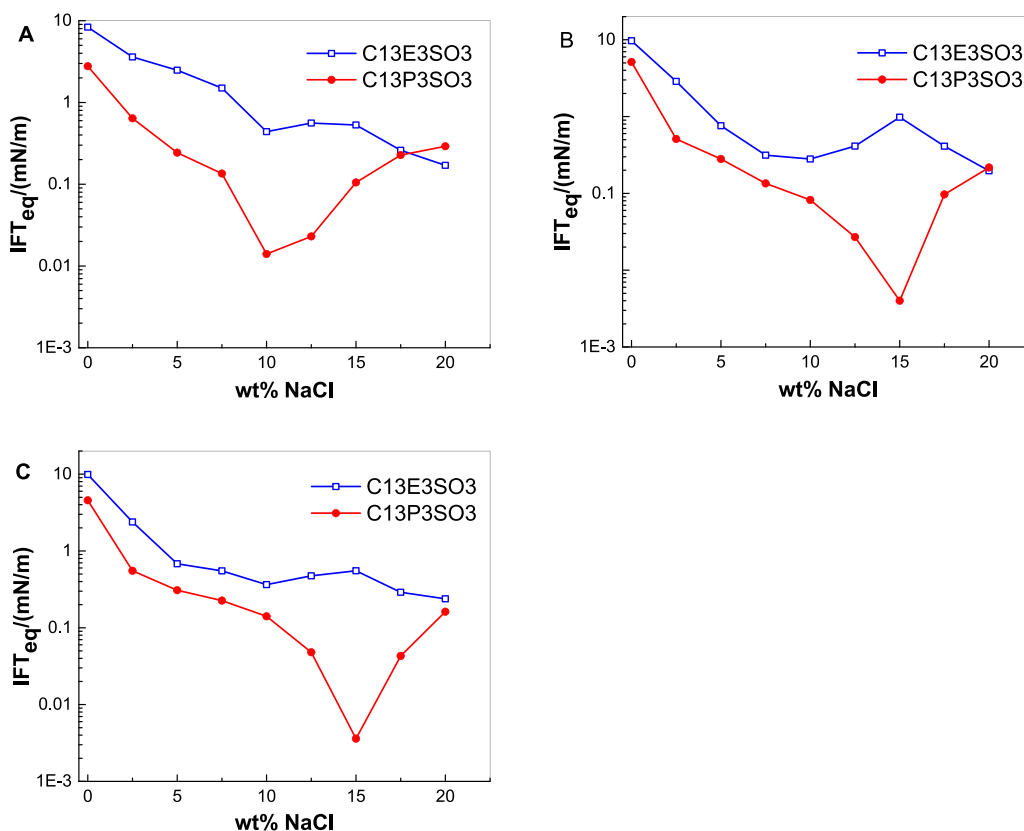


Figure 3. IFT_{eq} between *n*-octane and C13E3SO3 or C13P3SO3 solutions (A), *n*-decane and C13E3SO3 or C13P3SO3 solutions (B), and *n*-dodecane and C13E3SO3 or C13P3SO3 solutions (C) at different salinities.

Table 1. Cardinal Number of Hydrophilic Groups and Lipophilic Groups

functional groups	cardinal number
PO	-0.15
EO	0.33
-SO ₃ Na	11

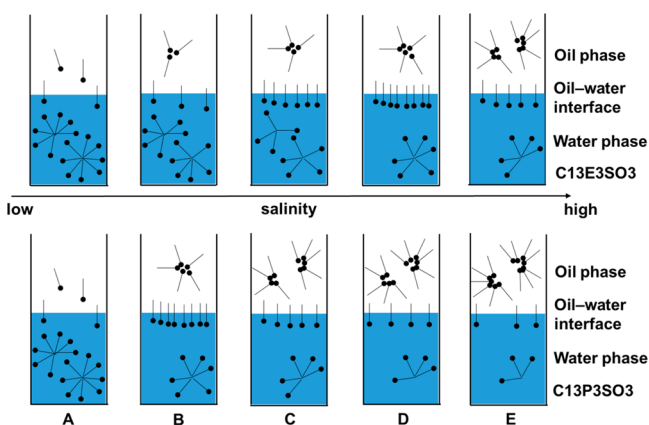


Figure 4. Effect of salinity on the distribution of the surfactant in oil/water phases at different salinities: lower than optimal salinity of C13P3SO3 (A), optimal salinity of C13P3SO3 (B), higher than optimal salinity of C13P3SO3 and lower than optimal salinity of C13E3SO3 (C), optimal salinity of C13E3SO3 (D), and higher than optimal salinity of C13E3SO3 (E).

$$R = \frac{A_{co} - A_{oo} - A_{ll}}{A_{cw} - A_{ww} - A_{hh}} \quad (1)$$

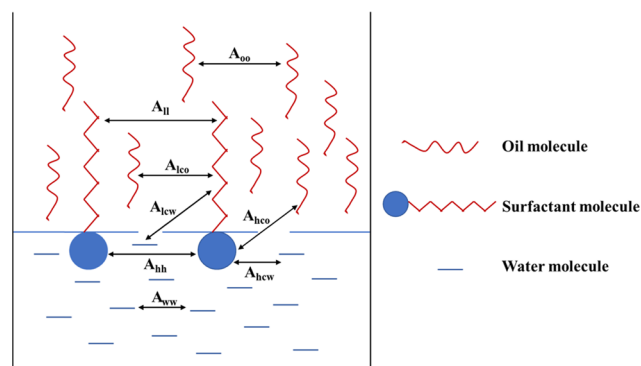


Figure 5. Interactions between different molecules at the oil/water interface.

When $R = 1$, the distribution of the surfactant at the oil–water interface reaches its optimal state, and the mutual effect among the oil phase, water phase, and amphiphilic region is in an equilibrium state. Under this condition, the IFT is the lowest. If one variable is changed, the hydrophilicity and lipophilicity of the surfactant will be altered and the oil–water system will deviate from its optimal state. However, in certain cases, if two variables are altered simultaneously, it is possible that the system could retain its optimal state. Such changes are identified as a compensation relationship. As shown in Figure 3, if the EO groups are displaced by PO groups, the molecule's lipophilicity will be improved and R will increase according to eq 1. To compensate for improvements in the molecule's lipophilicity as caused by the presence of PO groups, the salinity can be decreased to improve the molecule's hydro-

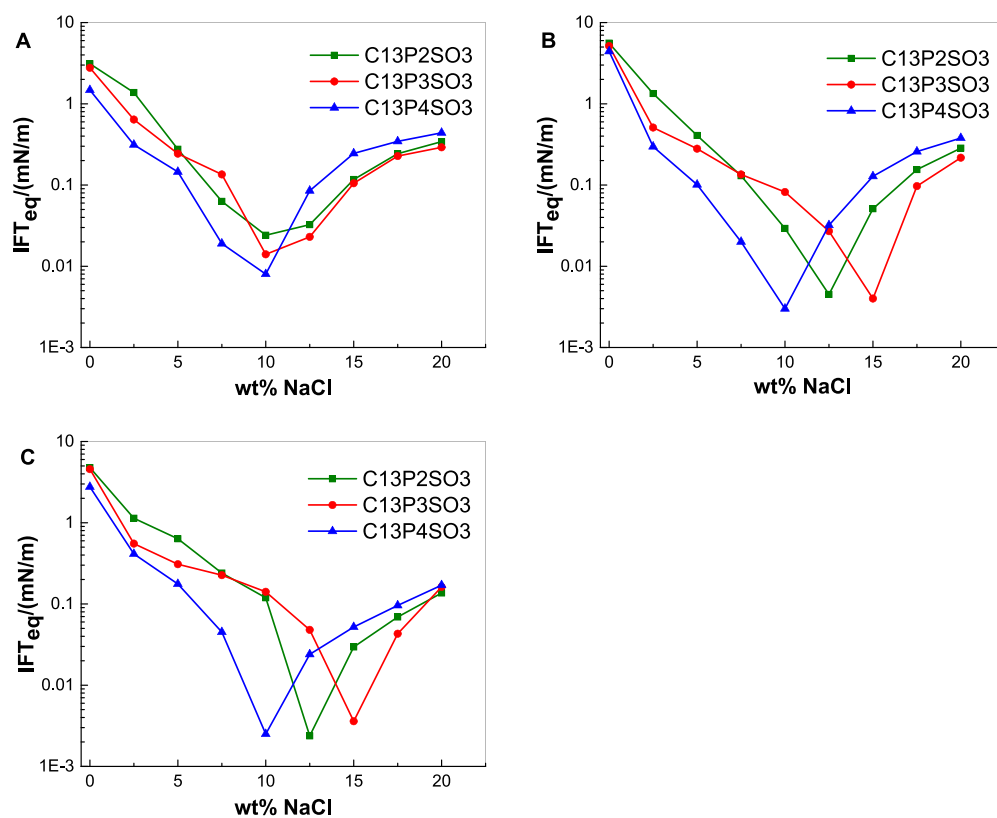


Figure 6. IFT_{eq} between *n*-octane and C13P n SO₃ solutions (A), *n*-decane and C13P n SO₃ solutions (B), and *n*-dodecane and C13P n SO₃ solutions (C) at different salinities.

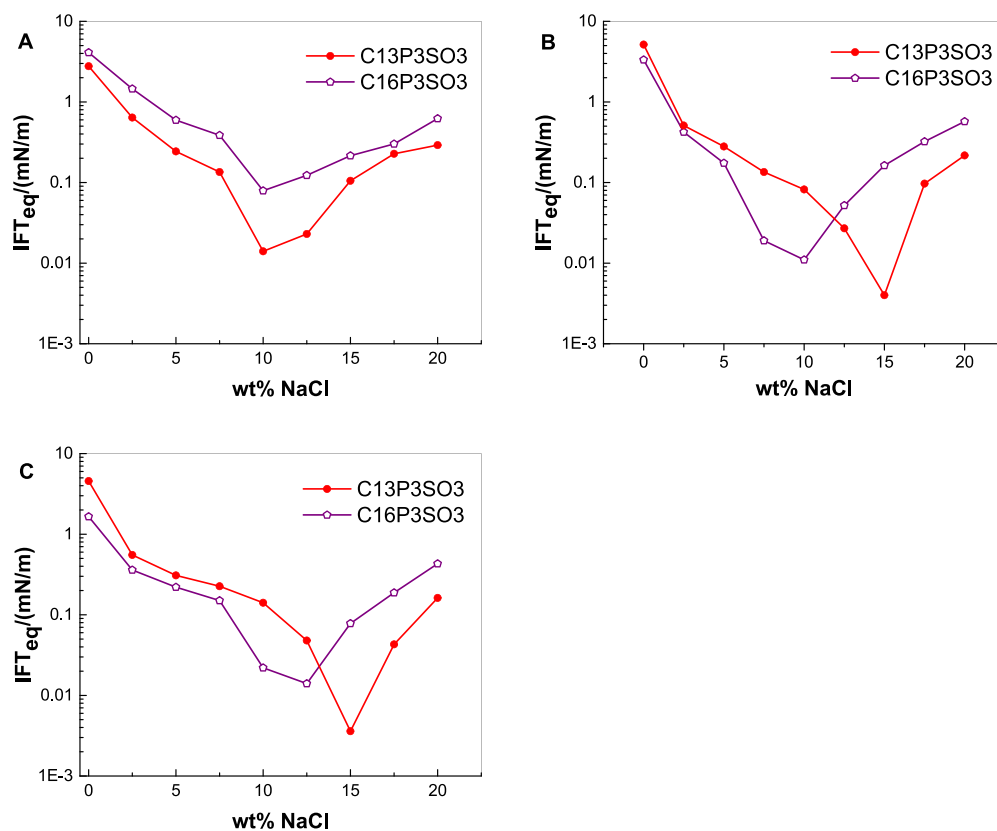


Figure 7. IFT_{eq} between *n*-octane and C13P3SO₃ or C16P3SO₃ solutions (A), *n*-decane and C13P3SO₃ or C16P3SO₃ solutions (B), and *n*-dodecane and C13P3SO₃ or C16P3SO₃ solutions (C) at different salinities.

Table 2. Optimal Salinity of Extended Surfactants and Ethoxylated Sulfonate

<i>n</i> -alkane	C13E3SO3	C13P2SO3	C13P3SO3	C13P4SO3	C16P3SO3
<i>n</i> -octane	≥20	10	10	10	10
<i>n</i> -decane	≥20	12.5	15	10	10
<i>n</i> -dodecane	≥20	12.5	15	10	12.5

phility, maintaining the oil–water system in its optimal state. Therefore, the optimal salinity of C13P3SO3 was lower than that of C13E3SO3 in this work.

Effects of the Number of PO Groups. Figure 6 shows the variation curves of the IFT_{eq} between *n*-alkanes and C13P n SO3 solutions at different salinities. For the same alkane, when the salinity is below a certain value, if the C13P n SO3 molecule contains more PO groups, the IFT_{eq} between *n*-alkanes and C13P n SO3 solutions is lower. Taking the oil phase of *n*-dodecane as an example, prior to the optimal salinity for C13P4SO3, the C13P4SO3 with the most PO groups in our experiments led to the lowest IFT_{eq} between *n*-alkanes and solutions. Further, in this case, the IFT_{eq} between *n*-alkanes and C13P3SO3 solutions is lower than the IFT_{eq} between *n*-alkanes and C13P2SO3 solutions. This result shows that the IFT_{eq} can decrease with increasing numbers of PO groups under low-salinity conditions. This can be explained by the fact that increasing the PON changed the oleophilic and hydrophilic properties of the surfactant and improved the aggregation capability of the surfactant to the oil phase before the optimal salinity.

Additionally, this result demonstrates that the optimal salinity of extended surfactants first increases and then decreases with increasing PON. Zeng et al.³⁶ found that the optimal salinity increased with increasing PON when studying the IFT between polyoxypropylene ether sulfate with lower numbers of PO groups and pure hydrocarbons. As previously reported, the optimal salinity decreased as the PON increased.^{28–31} In combination with the data presented in this paper, a law can be deduced, specifically, that the optimal salinity of extended surfactants is affected by PO groups. The optimal salinity first increases and then decreases with increasing PON for one type of extended surfactants. There is an appropriate PON keeping one type of extended surfactants with the highest optimal salinity. Salager's group³⁷ suggested that the first two to three PO groups in the extended surfactant are likely to be slightly hydrated and bent to accommodate some proximity of the interface for the first propylene oxide groups assembled closed to the oil/water interface. As a result, the improvement of the molecule's hydrophilicity by a few PO groups can be compensated by increasing the salinity to retain the system in its optimal state. Therefore, the presence of a few PO groups on the molecule can increase the optimal salinity. However, when PON reaches a certain value, the lipophilicity of the PO group comes into play. Then, increasing the PON can improve the lipophilicity of the molecule, which can be compensated by decreasing the salinity to retain the system's optimal state. Therefore, the optimal salinity decreases with increasing PON at values more than 4.

Effects of the Alkyl Chain Length. Figure 7 shows the IFT_{eq} variation curves between *n*-alkanes and solutions of extended surfactants with different alkyl chains at different salinities.

As shown in Figure 7, the IFT_{eq} between *n*-octane and C13P3SO3 solutions is lower than the IFT_{eq} between *n*-octane

and C16P3SO3 solutions over the whole range of experimental salinity. However, the IFT_{eq} between other *n*-alkanes (*n*-decane or *n*-dodecane) and C16P3SO3 solutions is lower than that between other *n*-alkanes (*n*-decane or *n*-dodecane) and C13P3SO3 solutions in the range of medium–low salinity, reversing in the range of high salinity. According to the assignment model, the presence of a relatively long lipophilic group has caused the distribution of the C16P3SO3 molecules among the oil and water phases to reach equilibrium more easily than the C13P3SO3 molecules. Therefore, in the range of medium–low salinity, C16P3SO3 has a stronger interfacial adsorption capability, which produces a lower IFT_{eq} between C16P3SO3 and either *n*-decane or *n*-dodecane. When the salinity is higher, the water solubility of C16P3SO3 decreases, leading to the dispersion of more C16P3SO3 molecules in the oil phase, whereas the distribution of C13P3SO3 molecules on the oil–water interface approaches equilibrium. The approach of C13P3SO3 molecules to an equilibrium distribution leads to a lower IFT_{eq} between *n*-alkanes and C13P3SO3 solutions than that between *n*-alkanes and C16P3SO3 solutions.

The range of the optimal salinity of C16P3SO3 is associated with the molecule's relatively long lipophilic group chain, which is lower than that of C13P3SO3 (i.e., a comparatively short lipophilic chain). This can be explained by a reason similar to that for the optimal salinity of C13P3SO3 being lower than that of C13E3SO3. Because the lipophilicity of C16P3SO3 is stronger than the lipophilicity of C13P3SO3, the salinity should be decreased to enhance the hydrophilicity of C16P3SO3 and compensate for the enhanced lipophilicity. It is also believed that the addition of salt can enhance the aggregation of surfactant molecules at the oil–water interface. When the system reaches the optimal salinity, the adsorption of the surfactant molecules at the oil–water interface reaches equilibrium and the IFT is the lowest. Because the C16P3SO3 molecules have a higher capability to transit to the oil–water interface than C13P3SO3 molecules, it is significantly easier for the C16P3SO3 solution to reach adsorption equilibrium at a lower salinity.

Effect of the Alkane Carbon Number on the Optimal Salinity. Table 2 shows the optimal salinity of ethoxylated sulfonates and extended surfactants. The optimal salinity increases with the alkane carbon number. For a given oil phase, every surfactant solution has a corresponding optimal salinity that optimizes the state of the system at a fixed surfactant concentration. Under this condition, $R = 1$. If the alkane carbon number of the oil phase increases, the intermolecular cohesive energy A_{oo} of the oil phase also increases, leading to a decrease of R . Accordingly, the compensation for the decrease of R can be promoted by raising the salt concentration, known as a hydrophilic–lipophilic compensation. Therefore, as the alkane carbon number of the oil phase is increased, the corresponding optimal salinity also increases. With increasing optimal salinity, it can be observed that the low-IFT regions of C13P3SO3 and C13E3SO3 shift to the right in Figure 3 and lead to an increase of the cross-salinity.

CONCLUSIONS

Based on the above discussion, the following conclusions can be drawn: (1) Compared with C13E3SO₃, C13P3SO₃ exhibits a better capacity to reduce the IFT when the salinity is less than the critical salinity, which increases with the alkane carbon number. However, C13P3SO₃ has a smaller optimal salinity than C13E3SO₃. (2) At a given salinity, the capacity to reduce the IFT of C13P_nSO₃ is improved with increasing numbers of PO groups. If there is no change in the oil phase, the optimal salinity of C13P_nSO₃ first increases and then decreases with increasing numbers of PO groups, which is a phenomenon first suggested here. (3) A cross-salinity also exists for extended surfactants with different alkyl chains. C16P3SO₃ has a better capacity to lower the interfacial tension than C13P3SO₃ at salinities below the critical salinity. The optimal salinity of C16P3SO₃ is lower than that of C13P3SO₃ for different *n*-alkanes. (4) For a given surfactant solution, alkane variation significantly affects the optimal salinity, which tends to increase with the alkane carbon number. Based on this finding, we can test the alkane carbon number of crude oils first, and then select the appropriate surfactants to be applied in enhancing oil recovery.

EXPERIMENTAL SECTION

Reagents. Surfactants used in this work are polyoxyethylene sulfonate and extended surfactants, including isotridecyl polyoxyethylene sulfonate, isotridecyl polyoxypropylene sulfonate, and hexadecyl polyoxypropylene sulfonate, which are summarized in Table 3 and were synthesized in our

Table 3. Surfactants Studied in This Work

name	chemical formula	% active ^a
C13E3SO ₃	C ₁₃ H ₂₇ -(EO) ₃ -SO ₃ Na	72.3
C13P2SO ₃	C ₁₃ H ₂₇ -(PO) ₂ -SO ₃ Na	71.6
C13P3SO ₃	C ₁₃ H ₂₇ -(PO) ₃ -SO ₃ Na	71.2
C13P4SO ₃	C ₁₃ H ₂₇ -(PO) ₄ -SO ₃ Na	69.5
C16P3SO ₃	C ₁₆ H ₃₃ -(PO) ₃ -SO ₃ Na	70.9

^a% Active: the active surfactant content determined by the direct two-phase titration procedure.³⁹

laboratory following the Strecker sulfonation procedure.³⁸ The oleic phase, *n*-octane, *n*-decane, and *n*-dodecane, and the sodium chloride (NaCl) were all of analytical purity and purchased from Sinopharm Chemical Reagent Co., Ltd. Deionized water was used for aqueous solution preparation.

Measurement of the Dynamic IFT. In this study, the dynamic IFTs between 0.1 wt % surfactant solutions and *n*-alkanes at different salinities were measured using an American Texas-500A spinning-drop interfacial tensiometer, equipped with a camera for image acquisition. All experiments were performed at 30.0 ± 0.1 °C.

A surfactant solution, including a specified amount of NaCl, was injected into the sample tube as the water phase; then, 1.5 μL of alkane was injected into the middle of the tube as the oil phase. The oil phase shape images at different times were obtained by an interfacial tensiometer. Figure 1 shows how the images of the oil droplet shape changed with time. Then, the images are processed through an image-processing tool developed by our lab to obtain the dynamic IFT according to eq 2.

$$\text{IFT} = \frac{\Delta\rho\omega^2r^3}{4} \quad (2)$$

where $\Delta\rho$, ω , and r are the difference in density between the oil and water phases, the angular velocity, and the minor axis semi-diameter of the droplet, respectively.

AUTHOR INFORMATION

Corresponding Authors

*E-mail: he7392337@163.com (W.H.).

*E-mail: gejijiang@163.com (J.G.).

ORCID

Weidong He: 0000-0001-8693-3538

Notes

The authors declare no competing financial interest.

ACKNOWLEDGMENTS

Financial support from the National Natural Science Foundation of China (51104170), the National High Technology Research and Development Program of China (2007BAE52B05), and the Supported by Program for New Century Excellent Talents in University from the Ministry of Education of China (NECT-07-0846) is greatly acknowledged.

REFERENCES

- Wang, H.; Cao, X.; Zhang, J.; Zhang, A. Development and Application of Dilute Surfactant-Polymer Flooding System for Shengli Oilfield. *J. Pet. Sci. Eng.* **2009**, *65*, 45–50.
- Robert, T.; Martel, R.; Conrad, S. H.; Lefebvre, R.; Gabriel, U. Visualization of TCE Recovery Mechanisms Using Surfactant-Polymer Solutions in a Two-Dimensional Heterogeneous Sand Model. *J. Contam. Hydrol.* **2006**, *86*, 3–31.
- Babadagli, T. Dynamics of Capillary Imbibition when Surfactant, Polymer, and Hot Water Are Used as Aqueous Phase for Oil Recovery. *J. Colloid Interface Sci.* **2002**, *246*, 203–213.
- Li, G.; Mu, J.; Li, Y.; Yuan, S. An Experimental Study on Alkaline/Surfactant/Polymer Flooding Systems Using Nature Mixed Carboxylate. *Colloids Surf., A* **2000**, *173*, 219–229.
- Wang, B.; Wu, T.; Li, Y.; Sun, D.; Yang, M.; Gao, Y.; Lu, F.; Li, X. The Effects of Oil Displacement Agents on the Stability of Water Produced from ASP (Alkaline/Surfactant/Polymer) Flooding. *Colloids Surf., A* **2011**, *379*, 121–126.
- Liang, Y.; Gao, G.; Shi, G.; Wang, G.; Li, J.; Zhao, Y. Progressing Cavity Pump Anti-scaling Techniques in Alkaline-Surfactant-Polymer Flooding in the Daqing Oilfield. *Pet. Explor. Dev.* **2011**, *38*, 483–490.
- Liu, Q.; Dong, M.; Yue, X.; Hou, J. Synergy of Alkali and Surfactant in Emulsification of Heavy Oil in Brine. *Colloids Surf., A* **2006**, *273*, 219–228.
- Liu, Q.; Dong, M.; Ma, S.; Tu, Y. Surfactant Enhanced Alkaline Flooding for Western Canadian Heavy Oil Recovery. *Colloids Surf., A* **2007**, *293*, 63–71.
- Dong, M.; Ma, S.; Liu, Q. Enhanced Heavy Oil Recovery Through Interfacial Instability: A Study of Chemical Flooding for Brintnell Heavy Oil. *Fuel* **2009**, *88*, 1049–1056.
- Foster, W. R. A Low-Tension Waterflooding Process. *J. Pet. Technol.* **1973**, *25*, 205–210.
- Wilson, P. M. D.; Brandner, C. F. Aqueous Surfactant Solutions Which Exhibit Ultralow Tensions at the Oil-Water Interface. *J. Colloid Interface Sci.* **1977**, *60*, 473–479.
- Healy, R. N.; Reed, R. L. Physicochemical Aspects of Microemulsion Flooding. *Soc. Pet. Eng. J.* **1974**, *14*, 491–501.
- Healy, R. N.; Reed, R. L.; Stenmark, D. G. Multiphase Microemulsion Systems. *Soc. Pet. Eng. J.* **1976**, *16*, 147–160.
- Bansal, V. K.; Shah, D. O. The Effect of Addition Ethoxylated Sulfonate on Salt Tolerance, Optimal Salinity, and Impedence

Characteristics of Petroleum Sulfonate Solutions. *J. Colloid Interface Sci.* **1978**, *65*, 451–459.

(15) Bansal, V. K.; Shah, D. O. The Effect of Ethoxylated Sulfonates on Salt Tolerance and Optimal Salinity of Surfactant Formulations for Tertiary Oil Recovery. *Soc. Pet. Eng. J.* **1978**, *18*, 167–172.

(16) Bruson, H. A. Water-Soluble Capillary-Active Sulphonates. US Patent US21484321939.

(17) Skauge, A.; Palmgren, O. *Phase Behavior and Solution Properties of Ethoxylated Anionic Surfactants*; SPE International Symposium on Oilfield Chemistry: Houston, TX, 1989; pp 355–366.

(18) Abe, M.; Schechter, D.; Schechter, R. S.; Wade, W. H.; Weerasooriya, U.; Yiv, S. Microemulsion Formation with Branched Tail Polyoxyethylene Sulfonate Surfactants. *J. Colloid Interf. Sci.* **1986**, *114*, 342–356.

(19) Miller, D. J.; von Halasz, S. P.; Schmidt, M.; Holst, A.; Pusch, G. Dual Surfactant Systems for Enhanced Oil Recovery at High Salinities. *J. Pet. Sci. Eng.* **1991**, *6*, 63–72.

(20) Aoudia, M.; Al-Maamari, R. S.; Nabipour, M.; Al-Bemani, A. S.; Ayatollahi, S. Laboratory Study of Alkyl Ether Sulfonates for Improved Oil Recovery in High Salinity Carbonate Reservoirs: A Case Study. *Energy Fuels* **2010**, *24*, 3655–3660.

(21) Gale, W. W.; Puerto, M. C.; Ashcraft, T. L.; Saunders, R. K.; Reed, R. L. Propoxylated Ethoxylated Surfactants and Method of Recovering Oil Therewith. US Patent US42934281981.

(22) Miñana-Perez, M. M.; Graciaa, A.; Lachaise, J.; Salager, J. L. Solubilization of Polar Oil with Extended Surfactants. *Colloids Surf., A* **1995**, *100*, 217–224.

(23) Pérez, M. M.; Salager, J. -L.; Miñana-Pérez, M.; Graciaa, A.; Lachaise, J. *Colloid Polym. Sci.* **1995**, *177* 179, 1007.

(24) Jayanti, S.; Britton, L.; Dwarakanath, V.; Pope, G. A. Laboratory Evaluation of Custom-Designed Surfactants to Remediate NAPL Source Zones. *Environ. Sci. Technol.* **2002**, *36*, 5491–5497.

(25) Charoensaeng, A.; Sabatini, D. A.; Khaodhiar, S. Solubilization and Adsorption of Polar and Nonpolar Organic Solutes by Linker Molecules and Extended Surfactants. *J. Surfactants Deterg.* **2009**, *12*, 209–217.

(26) Witthayapanyanon, A.; Phan, T. T.; Heitmann, T. C.; Harwell, J. H.; Sabatini, D. A. Interfacial Properties of Extended-Surfactant-Based Microemulsions and Related Macroemulsions. *J. Surfactants Deterg.* **2010**, *13*, 127–134.

(27) Do, L. D.; Witthayapanyanon, A.; Harwell, J. H.; Sabatini, D. A. Environmentally Friendly Vegetable Oil Microemulsions Using Extended Surfactants and Linkers. *J. Surfactants Deterg.* **2009**, *12*, 91–99.

(28) Phan, T. T.; Attaphong, C.; Sabatini, D. A. Effect of Extended Surfactant Structure on Interfacial Tension and Microemulsion Formation with Triglycerides. *J. Am. Oil Chem. Soc.* **2011**, *88*, 1223–1228.

(29) Witthayapanyanon, A.; Acosta, E. J.; Harwell, J. H.; Sabatini, D. A. Formulation of Ultralow Interfacial Tension Systems Using Extended Surfactants. *J. Surfactants Deterg.* **2006**, *9*, 331–339.

(30) Liu, X.; Zhao, Y.; Li, Q.; Niu, J. Surface Tension, Interfacial Tension and Emulsification of Sodium Dodecyl Sulfate Extended Surfactant. *Colloids Surf., A* **2016**, *494*, 201–208.

(31) He, Z.; Zhang, M.; Fang, Y.; Jin, G.; Chen, J. Extended Surfactants: A Well-Designed Spacer to Improve Interfacial Performance through a Gradual Polarity Transition. *Colloids Surf., A* **2014**, *450*, 83–92.

(32) Talley, L. D. Hydrolytic Stability of Alkylethoxy Sulfates. *SPE Reservoir Eng.* **1988**, *3*, 235–242.

(33) Guo, L.; Liu, Y.; Hu, S.; Xu, Z.; Gong, Q.; Zhang, L.; Zhang, L. Dynamic Interfacial Tensions of Alkyl Alcohol Polyoxypropylene-Oxyethylene Ether Sulfonate Solutions. *J. Pet. Sci. Eng.* **2016**, *141*, 9–15.

(34) Zhao, Z.; Bi, C.; Li, Z.; Qiao, W.; Cheng, L. Interfacial Tension between Crude Oil and Decylmethylnaphthalene Sulfonate Surfactant Alkali-Free Flooding Systems. *Colloids Surf., A* **2006**, *276*, 186–191.

(35) Shen, Z.; Wang, G. T. *Colloid and surface Chemistry*; Chemical Industry Press: Beijing, 1997; pp 362.

(36) Zeng, J.; Ge, J.; Zhang, G.; Liu, H.; Wang, D.; Zhao, N. Synthesis and Evaluation of Homogeneous Sodium Hexadecyl Polyoxypropylene Ether Sulfates. *J. Dispersion Sci. Technol.* **2010**, *31*, 307–313.

(37) Forgiarini, A. M.; Scorzza, C.; Velásquez, J.; Vejar, F.; Zambrano, E.; Salager, J. L. Influence of the Mixed Propoxy/Ethoxy Spacer Arrangement Order and of the Ionic Head Group Nature on the Adsorption and Aggregation of Extended Surfactants. *J. Surfactants Deterg.* **2010**, *13*, 451–458.

(38) He, W.; Li, R.; Ge, J.; Zhang, G.; Li, N. The Synthesis and Interfacial Tension Determination of Octylphenol Polyoxyethylene Ether Sulfonate. *Petrochem. Univ.* **2010**, *23*, 20–25.

(39) Surface active agents-Detergents-Determination of anionic-active matter by manual or mechanical direct two-phase titration procedure. ISO 2271:1989.